The Journal of Physiology

# Feto- and utero-placental vascular adaptations to chronic maternal hypoxia in the mouse

Lindsay S. Cahill[1], Monique Y. Rennie[1], Johnathan Hoggarth[1], Lisa X. Yu[1], Anum Rahman[1,2], John C. Kingdom[3,4], Mike Seed[5], Christopher K. Macgowan[2,6] and John G. Sled[1,2,3,6]

[1] *Mouse Imaging Centre, The Hospital for Sick Children, Toronto, Ontario, Canada*
[2] *Department of Medical Biophysics, University of Toronto, Toronto, Ontario, Canada*
[3] *Department of Obstetrics and Gynecology, University of Toronto, Toronto, Ontario, Canada*
[4] *Lunenfeld-Tanenbaum Research Institute, Mount Sinai Hospital, Toronto, Ontario, Canada*
[5] *Division of Cardiology, Department of Paediatrics, The Hospital for Sick Children, Toronto, Ontario, Canada*
[6] *Translational Medicine, The Hospital for Sick Children, Toronto, Ontario, Canada*

**Key points**

- Chronic fetal hypoxia is one of the most common complications of pregnancy and is known to cause fetal growth restriction.
- The structural adaptations of the placental vasculature responsible for growth restriction with chronic hypoxia are not well elucidated.
- Using a mouse model of chronic maternal hypoxia in combination with micro-computed tomography and scanning electron microscopy, we found several placental adaptations that were beneficial to fetal growth including capillary expansion, thinning of the inter-haemal membrane and increased radial artery diameters, resulting in a large drop in total utero-placental vascular resistance.
- One of the mechanisms used to achieve the rapid increase in capillaries was intussusceptive angiogenesis, a strategy used in human placental development to form terminal gas-exchanging villi.
- These results contribute to our understanding of the structural mechanisms of the placental vasculature responsible for fetal growth restriction and provide a baseline for understanding adaptive physiological responses of the placenta to chronic hypoxia.

**Abstract** The fetus and the placenta in eutherian mammals have a unique set of compensatory mechanisms to respond to several pregnancy complications including chronic maternal hypoxia. This study examined the structural adaptations of the feto- and utero-placental vasculature in an experimental mouse model of chronic maternal hypoxia (11% $O_2$ from embryonic day (E) 14.5–E17.5). While placental weights were unaffected by exposure to chronic hypoxia, using micro-computed tomography, we found a 44% decrease in the absolute feto-placental arterial vascular volume and a 30% decrease in total vessel segments in the chronic hypoxia group compared to control group. Scanning electron microscopy imaging showed significant expansion of the capillary network; consequently, the interhaemal membrane was 11% thinner to facilitate maternal–fetal exchange in the chronic hypoxia placentas. One of the mechanisms for the rapid capillary expansion was intussusceptive angiogenesis. Analysis of the utero-placental arterial tree showed significant increases (24%) in the diameter of the radial arteries, resulting in a decrease in the total utero-placental resistance by 2.6-fold in the mice exposed to chronic maternal hypoxia. Together these adaptations acted to preserve placental weight whereas fetal weight was decreased.

(Received 29 June 2017; accepted after revision 25 August 2017; first published online 1 September 2017)
**Corresponding author** L. S. Cahill: Mouse Imaging Centre, The Hospital for Sick Children, 25 Orde Street, Toronto, Ontario, Canada M5T 2H7. Email: lindsay.cahill@sickkids.ca

**Abbreviations** CT, computed tomography; SEM, scanning electron microscopy; VEGF, vascular endothelial growth factor.


DOI: 10.1113/JP274845

## Introduction

Chronic fetal hypoxia is one of the most common complications of pregnancy and is potentially associated with a variety of maternal conditions including pre-eclampsia, gestational diabetes and maternal heart disease (Giussani, 2016). The fetus has a unique set of compensatory mechanisms to maintain oxygen delivery to the fetus in the face of reduced oxygen supply, including the ability to bind greater concentrations of oxygen in fetal haemoglobin (Martin, 2008), shunts in the fetal circulation to allow more oxygenated blood to be directed to the organs most prone to damage (i.e. brain and heart) (Cohn *et al.* 1974; Gleason *et al.* 1990; Pearce, 2006), the ability to limit fetal oxygen consumption by decreasing fetal heart rate and suspending fetal breathing movements (Boddy *et al.* 1974), and the ability of fetal haemoglobin to continue to release oxygen at low haemoglobin oxygen saturation levels. The placenta's role in the response to chronic hypoxia has primarily been investigated in high altitude pregnancies. These studies have shown that the feto-placental vasculature adapts to hypoxia by increasing villous capillary density (Alia *et al.* 1996; Tissot van Patot *et al.* 2003). Consequently, the diffusion barrier between maternal and fetal circulations thins to increase the exchange of oxygen and nutrients (Mayhew, 1998). However, opposing these adaptations is a reduced remodelling of the utero-placental spiral arteries (Zamudio, 2003). The overall response to pregnancy at high altitude is therefore variable, especially for women not normally resident at high altitude (Moore *et al.* 2004; Wilson *et al.* 2007).

The effects of chronic hypoxia in pregnancy have often been studied using animal models housed in specialized hypoxia chambers to mimic high altitude (for review, see Jang *et al.* 2015). While in high altitude pregnancies the placenta develops entirely under low oxygen conditions, animal models allow us to study the effects of specific windows of hypoxia on fetal and placental development. It should also be noted that maternal (or population-wide) adaptations prior to pregnancy are a confound in investigating chronic hypoxia in high altitude pregnancies. Studies using mouse models of chronic maternal hypoxia have reported decreased fetal weight (Gortner *et al.* 2005; Ream *et al.* 2008; Tomlinson *et al.* 2010; Cuffe *et al.* 2014; Rueda-Clausen *et al.* 2014) and altered placental development, specifically decreased labyrinth blood spaces (Cuffe *et al.* 2014; Higgins *et al.* 2016). However, the structural adaptations of the placental vasculature responsible for chronic maternal hypoxia that induces fetal growth restriction are not well elucidated. The mouse reproduces many of the features of human pregnancy (Georgiades *et al.* 2002; Mu & Adamson, 2006; Cox *et al.* 2009) and has enabled detailed analysis of placental adaptations to pregnancy complications (Coan *et al.* 2008; Bainbridge *et al.* 2012; Rennie *et al.* 2015). In human pregnancies, biopsies of the utero-placental circulation are usually limited to a small portion of the vascular bed (Lyall, 2005). As a result, little is known about the structural changes of the vessels upstream of the spiral arteries including the radial arteries, known to be the largest contributors to total utero-placental resistance (Rennie *et al.* 2016). Advanced 3D imaging of the murine placenta using X-ray micro-computed tomography (micro-CT) allow us to perform a detailed analysis of the entire utero- and feto-placental arterial circulations (Rennie *et al.* 2014*a*).

In the present study, we investigated the changes in geometry and resistance within the feto- and utero-placental vascular trees in placentas following exposure to chronic, late gestation maternal hypoxia in pregnant mice. Capillary remodelling and inter-haemal membrane thickness were assessed using scanning electron microscopy (SEM) and stereological techniques.

## Methods

### Ethical approval

Experimental procedures were approved by the Animal Care Committee of The Centre for Phenogenomics, conducted in accordance with guidelines established by the Canadian Council on Animal Care and complied with the ARRIVE guidelines.

### Animals

CD-1 mice were purchased from Charles River Laboratories (St Constant, QC, Canada). Males were mated in-house with virgin females aged 8–14 weeks and the morning that a vaginal copulation plug was detected was designated embryonic day (E) 0.5. Mice were housed in a standard cage with *ad libitum* access to food and water.

### Chronic hypoxia protocol

Pregnant mice were randomized to prenatal chronic hypoxia (11% $O_2$) or normoxia (21% $O_2$) conditions from E14.5 to E17.5 (E18.5 is term in this strain of mice). Mice assigned to the prenatal chronic hypoxia group were housed in a standard cage that at E14.5 was placed inside a sealed acrylic chamber (medium A-chamber, 30 inches W × 20 inches D × 20 inches H, Biospherix, NY, USA). This chamber maintained an internal concentration of oxygen at 11% by regulating nitrogen infusion. 200 grams of soda lime (Alfa Aesar, Ward Hill, MA, USA) was placed in the lower level of the chamber to scavenge excess $CO_2$. All animals were killed at E17.5 using cervical dislocation.

### Injection of contrast agent

The E17.5 arterial feto-placental vasculature was prepared for micro-CT (8 placentas from 4 control dams and 8 placentas from 3 chronic hypoxia dams) and SEM imaging (6 placentas from 3 control dams and 5 placentas from 4 chronic hypoxia dams) as described previously (Rennie *et al.* 2014*b*, 2015). Briefly, E17.5 conceptuses were surgically exposed and a double lumen cannula was inserted into the umbilical artery (Whiteley *et al.* 2006). Blood was cleared from the vasculature using heparinized saline containing xylocaine. For micro-CT imaging, MV-122 Microfil (Flow Tech Inc., Carver, MA, USA) was then manually infused until it was seen entering the capillary bed. For SEM imaging, methyl methacrylate (Batson's no. 17, Polysciences, Warrington, PA, USA) was manually infused, filling all feto-placental vessels, until it was seen exiting the umbilical vein. The umbilical vessels were ligated to maintain pressure during polymerization of the contrast agent. Placentas for micro-CT imaging were immersed in formalin and later mounted in agar. Methyl methacrylate perfused placentas were immersed in 20% potassium hydroxide for 24–48 h, which macerated all tissue surrounding the casts.

In a separate cohort of mice, the utero-placental vasculature (7 placentas from 4 control dams and 8 placentas from 4 chronic hypoxia dams) was perfused with HV-122 Microfil (Flow Tech Inc.) via cannulation of the descending aorta using previously established methods (Whiteley *et al.* 2006; Rennie *et al.* 2014*b*). Pump infusion was stopped when the bright yellow colour of the contrast agent was seen entering the utero-placental microvasculature of the exposed uterus and the system was pressurized to 20 mmHg (i.e. micro-vascular pressure) while the compound polymerized. This pressure was chosen to match the known pressure in the capillaries (Bohlen & Gore, 1977) and therefore avoid damage from over-pressurization. The uterus was then removed, immersed in formalin, and uterine segments later mounted in agar for micro-CT imaging. The entire utero-placental circulation was perfused for each dam and placentas for analysis were selected based on complete filling of the arterial vasculature. Implantation sites were chosen randomly from the left and right uterine horns and from the cervical and ovarian end of the uterine horn. The normoxic control group data has been previously published (Rennie *et al.* 2016).

### Micro-CT imaging and vascular segmentation

3D datasets were acquired for feto-placental and utero-placental contrast-enhanced specimens with the surrounding tissue still intact using a Bruker Skyscan 1272 micro-CT scanner (Bruker Skyscan, Belgium). The scanning protocol for the feto-placental specimens was as follows: with the X-ray source at 50 kV and 201 $\mu$A, the specimen was rotated 360 deg in 0.2 deg increments, generating 1800 views which were reconstructed into data blocks with a 7.1 $\mu$m voxel size. For the utero-placental specimens, with the X-ray source at 50 kV and 201 $\mu$A, the specimen was rotated 360 deg in 0.4 deg increments, generating 900 views which were reconstructed into data blocks with a 16.4 $\mu$m voxel size. Vascular surface renderings were generated from micro-CT data to visualize the arterial vasculature.

The feto-placental arterial vasculature was automatically segmented, identifying vessel segments and bifurcations using an algorithm as described in detail previously (Rennie *et al.* 2011). The algorithm returned the centre lines of a connected vessel tree and a tubular model for which the lengths, diameters, and connectivity of each vessel segment were known. Measurements of vessel segment numbers and the distribution of vessel diameters were extracted from the resultant tubular models for all vessels $>35$ $\mu$m (Rennie *et al.* 2011, 2012). Diameter and length measurements of the utero-placental vascular tree were made using digital calipers in the Amira software package (Visage Imaging, San Diego, CA, USA) (Rennie *et al.* 2016). Diameter measurements were made and then averaged from three or more sites along the uterine artery, radial arteries and canals, and at 15 or more sites along the spiral arteries to account for the larger variation in diameters in these spiraling vessels (Rennie *et al.* 2016).

### Resistance calculations

Utero-placental vascular resistance was calculated as described previously (Rennie *et al.* 2016). Briefly, the calculations assume laminar flow, Poiseuille's law, conservation of mass and equations for resistances in series and parallel. The total resistance of each analysed utero-placental vascular tree was calculated from the number and the average diameter and length of the radial arteries, spiral arteries, maternal canals and maternal canal branches in that tree.

### Immunohistological detection of hypoxia and fetal capillary endothelium

In a separate series of mice, the hypoxia marker pimonidazole hydrochloride (Hypoxyprobe-1, Burlington, MA, USA) was injected intraperitoneally (60 mg kg$^{-1}$) at E17.5 (4 control dams and 4 chronic hypoxia dams). The dams were returned to their normoxic or hypoxic environments following the injection. Following previously established protocols for pimonidazole immunostaining of mouse embryos (Kulandavelu *et al.* 2013), the dam was killed by cervical dislocation 90 min post-injection and mid-horn placentas

(2 per dam) were collected, processed, and sectioned (5 $\mu$m thickness). Placental midline sections were stained to detect placental hypoxia using Hypoxyprobe or stained to quantify interhaemal membrane thickness with CD34 using anti-mouse CD34 antibody (Serotec, 1:100) following previously established protocols (Rennie *et al.* 2012). Stained slides were scanned at high resolution to facilitate quantitative analysis.

### Immunohistological analysis and stereology

Fractional area stained for Hypoxyprobe of each placenta was computed via use of the colour thresholding and area fraction tools in ImageJ (National Institutes of Health, Bethesda, MD, USA). A negative control slide (secondary antibody only) was analysed similarly and its fractional area staining subtracted from all other datasets to account for any erroneous background staining. Interhaemal membrane thickness was measured using ImageJ from a midline section stained for CD34 using stereological principles and corrected for shrinkage, as has previously been described in detail (Coan *et al.* 2004; Rennie *et al.* 2012). Approximately 100 measurements were made per placenta using the ImageJ grid function using line probes with random offset (area per point: 3000 pixels$^2$) and the orthogonal intercept method.

### Scanning electron microscopy

The complete feto-placental vasculature infused with methyl methacrylate was viewed using a PEI XL30 scanning electron microscope (FEI Systems Canada, Toronto, ON, Canada). Magnifications ranged from (35× to 2000×). Tuft length of each placenta was measured directly from SEM images acquired at 200× magnification using ImageJ. Capillary diameter measurements were made from SEM images (magnification of 1000×) using stereological principles and the ImageJ grid function as described above, using a grid of crosshairs with a grid size of 2000 microns/point. Approximately 25 measurements of capillary diameter were made per placenta.

### Statistical analysis

All statistical tests were performed using the *R* statistical software (www.r-project.org). Data from each group of animals are reported as the means ± 95% confidence intervals and analysed using Student's *t* tests to compare groups. Litter means were used for statistical analysis of fetal and placental weights. We used a linear model to determine whether total vessel segments depended on fetal weight with main effects of group and fetal weight, and an interaction term between the two. A value of $P < 0.05$ was taken to be significant.

## Results

### Maternal, fetal and placental weights and measurements

There was no difference in maternal weight prior to mice being randomly assigned at E14.5 to either the chronic hypoxia or control group (control 44 g (CI: 39–49) *vs.* chronic hypoxia 44 g (CI: 41–47)). However, following maternal exposure to hypoxia during late gestation (E14.5–E17.5), the dams ($N = 10$) gained significantly less weight compared to controls ($N = 6$) (control 10 g (CI: 6–14) *vs.* chronic hypoxia 1 g (CI: 0–2), $P < 0.0001$) (Fig. 1*A*). In addition, the fetuses exposed to chronic maternal hypoxia ($N = 12$) weighed 25% less than controls ($N = 12$) (control 1.3 g (CI: 1.1–1.5) *vs.* chronic hypoxia 1.0 g (CI: 0.9–1.1), $P < 0.005$) at E17.5 (Fig. 1*B*), indicating that the hypoxia-exposed fetuses failed to reach their growth potential. In contrast, placental weights (control 0.17 g (CI: 0.15–0.19) *vs.* chronic hypoxia 0.15 g (CI: 0.14–0.16), $P = 0.1$) (Fig. 1*C*) were unaffected by exposure to chronic maternal hypoxia. The feto-placental weight ratio, a measure of placental efficiency (Perry *et al.* 1995), was significantly lower in the chronic hypoxia group (control 7.8 (CI: 6.4–9.2) *vs.* chronic hypoxia 6.3 (CI: 5.5–7.1), $P = 0.04$), consistent with fetal growth restriction (Hayward *et al.* 2016). While there was no difference in the diameter of the umbilical artery, the length of the umbilical cord was significantly shorter in the hypoxia-exposed placentas *vs.* controls (control 13.0 mm (CI: 12.1–13.9) *vs.* chronic hypoxia 10.6 mm (CI: 9.6–11.6), $P < 0.001$) (Fig. 1*D*).

Pimonidazole hydrochloride staining of the placental tissue showed no evidence of significant placental hypoxia at E17.5 in either the labyrinth or junctional zone of the chronic hypoxia or control group (Fig. 2). The absence of further hypoxia beyond that seen under control conditions in the placenta indicates that the placental tissues are intrinsically capable of compensating for the reduced oxygen conditions.

### Hypoxia-exposed phenotype of the feto-placental arterial tree

The geometry of the feto-placental arterial vasculature at E17.5 was visualized using surface renderings of the micro-CT data for control ($n = 8$) and chronic hypoxia ($n = 8$) placentas (Fig. 3*A* and *B*). The depth (control 2.1 mm (CI: 1.9–2.3) *vs.* chronic hypoxia 2.2 mm (CI: 2.0–2.4)) and span (control 6.8 mm (CI: 6.6–7.0) *vs.* chronic hypoxia 6.4 mm (CI: 6.0–6.8)) of the arterial tree were not significantly different between the groups. However, compared to the arterial tree in the control group, there was a significant decrease in the vascular volume of the chronic hypoxia placentas (control 7.9 mm$^3$

(CI: 5.2–10.6) *vs.* chronic hypoxia 4.4 $mm^3$ (CI: 2.3–6.5); $P < 0.05$) (Fig. 3*C*). This was supported by vascular segmentation which revealed that there was a significant decrease in the total number of vessel segments in the feto-placental arterial tree (control 6900 (CI: 5800–8000) vessels *vs.* chronic hypoxia 4800 (CI: 3000–6600) vessels; $P < 0.05$) (Fig. 3*D*). To further explore if this difference was confined to a specific part of the placenta, the numbers of vessel segments were determined within diameter ranges corresponding to approximate anatomic locations within the tree; arterioles 35–75 $\mu$m, intraplacental arteries 75–150 $\mu$m and chorionic plate arteries >200 $\mu$m (Rennie *et al.* 2012). Arteriole vessel number was decreased by 1.4-fold (control 6000 (CI: 5000–7000) *vs.* chronic hypoxia 4200 (CI: 2600–5800); $P < 0.05$) and the intraplacental artery vessel number was decreased by 1.6-fold (control 860 (CI: 690–1030) *vs.* chronic hypoxia 530 (CI: 310–750); $P < 0.05$) whereas no changes in the chorionic plate arteries were observed. Interestingly, the fetal weight showed a significant positive dependence on total number of vessel segments ($P < 0.0001$, adjusted $R^2 = 0.74$) that did not differ between chronic hypoxia and control groups (Fig. 3*E*).

We next used SEM images to examine differences between groups in the placental vasculature at the capillary level (Fig. 4*A*). The average length of the capillary tufts (control 0.68 mm (CI: 0.64–0.72) *vs.* chronic hypoxia 0.8 mm (CI: 0.7–0.9); $P < 0.05$) and

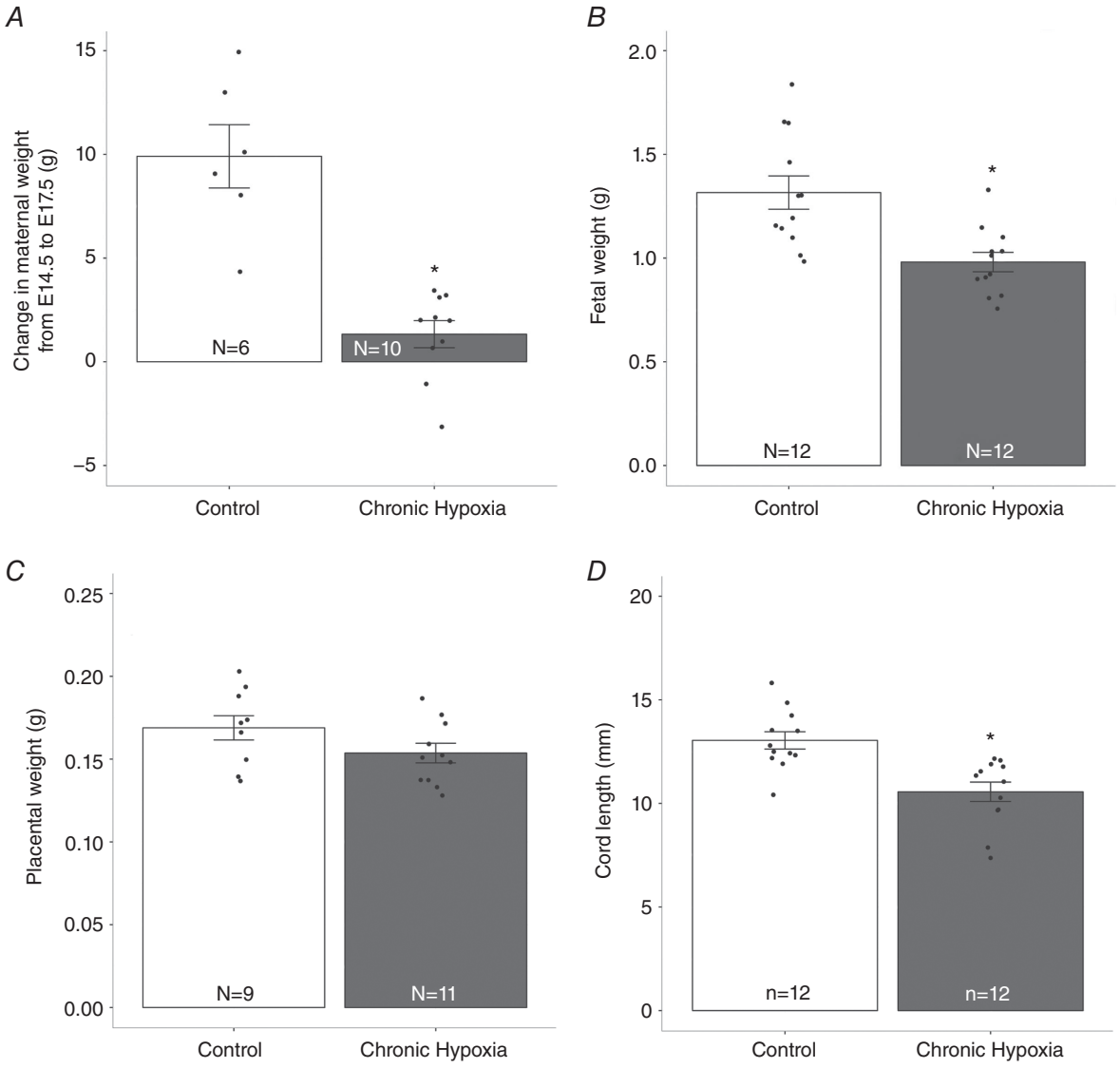


**Figure 1. The effects of chronic maternal hypoxia on maternal, fetal and placental parameters**
Change in maternal weight from E14.5 to E17.5 (g; *A*), fetal weight (g; *B*), placental weight (g; *C*) and umbilical cord length (mm; *D*) for chronic hypoxia (filled bars) compared to controls (open bars). Data shown as means ± 95% confidence intervals (CI). *N* refers to the number of dams and *n* refers to the number of placentas. *$P < 0.005$.

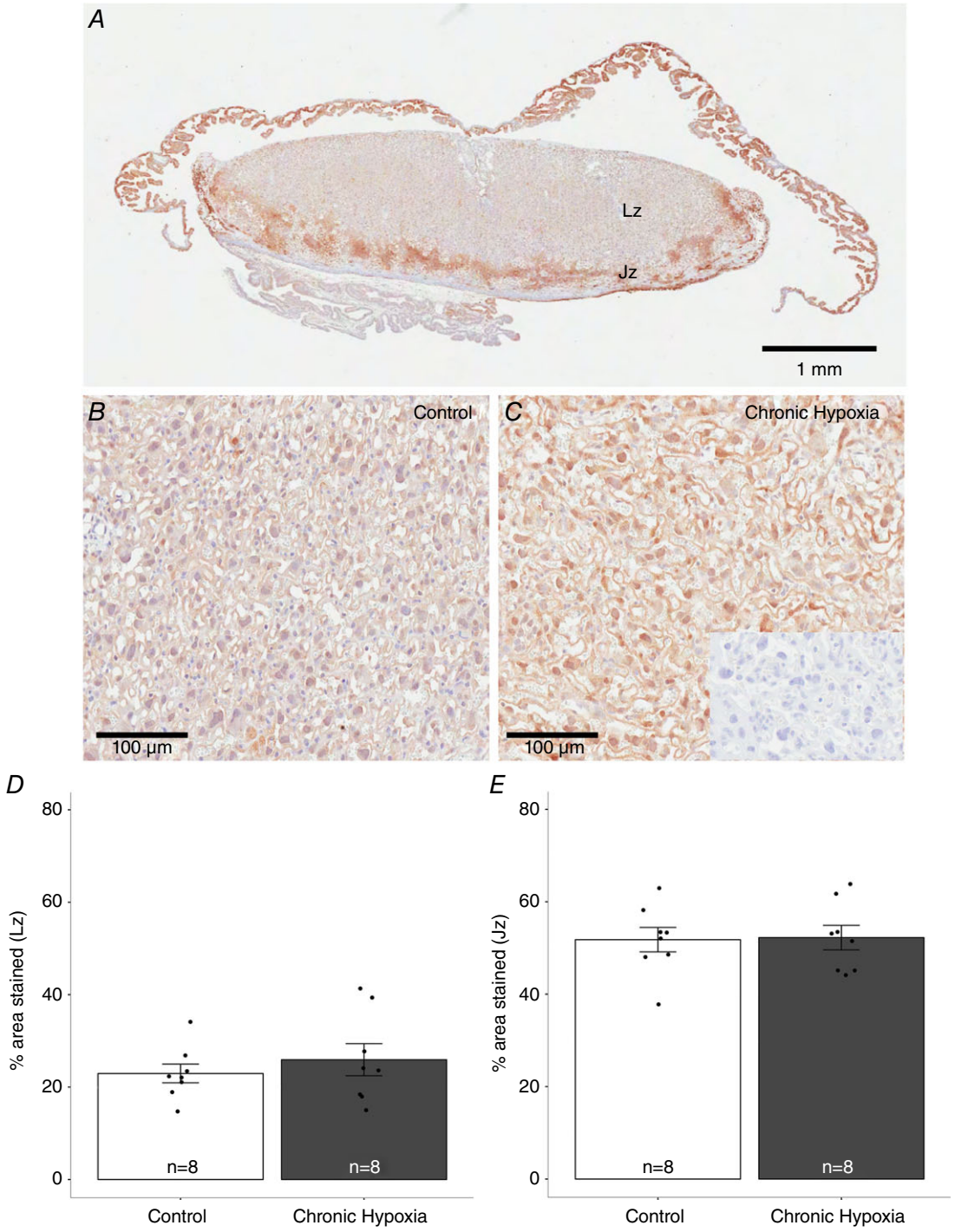


**Figure 2. Detection of placental hypoxia via Hypoxyprobe staining**
*A*, representative midline section from a control placenta exhibits mild Hypoxyprobe staining of the labryinth zone (Lz) and more pronounced staining of the avascular junctional zone (Jz). Scale = 1 mm. Images of the Lz in the control (*B*) and chronic hypoxia (*C*) groups revealed a similar staining pattern. Inset in *C* is a negative control (secondary antibody only). Scale = 100 $\mu$m. The percentage area of positive Hypoxyprobe staining for the labryinth zone (*D*) and junctional zone (*E*) for chronic hypoxia (filled bars) compared to controls (open bars). Data shown as means ± 95% confidence intervals. *n* refers to the number of placentas. [Colour figure can be viewed at wileyonlinelibrary.com]

the average capillary diameter (control 7.3 $\mu$m (CI: 6.4–8.2) *vs.* chronic hypoxia 11.0 $\mu$m (CI: 9.4–12.6); $P < 0.0005$) were significant greater in the chronic hypoxia-exposed placentas compared to the controls (Fig. 4*B* and *C*), indicating that chronic maternal hypoxia triggers capillary expansion to increase the surface area available for exchange of oxygen and nutrients. Another compensatory mechanism to facilitate maternal–fetal exchange is thinning of the interhaemal membrane. In the chronic hypoxia placentas, the interhaemal membrane was 11% thinner compared to controls (control 3.4 $\mu$m (CI: 3.2–3.6) *vs.* chronic hypoxia 3.0 $\mu$m (CI: 2.8–3.2); $P < 0.005$) (Fig. 4*D*). Interestingly, the SEM images of the chronic hypoxia placentas showed evidence of intussusceptive angiogenesis, identified by distinctive intussusceptive pillars (indicated by arrowheads in Fig. 4*E*) (Mentzer & Konerding, 2014). These are analogous in humans to the formation of terminal villi within mature intermediate villi in the third trimester (Kingdom & Kaufmann, 1997).

## Hypoxia-exposed phenotype of the utero-placental arterial tree

The structure of the utero-placental vascular tree was similar between groups (Fig. 5*A* and *B*). The uterine artery directly supplied two pre-placental radial arteries which branched into five to eight spiral arteries and converged into two to four maternal canals. The diameters of the uterine artery, pre-myometrial radial arteries, spiral arteries and canals were the same between groups. However, the first and second order radial arteries were significantly larger in diameter in the chronic hypoxia placentas compared to controls (first order radial arteries: control 0.13 mm (CI: 0.11–0.15) *vs.* chronic hypoxia 0.16 mm (CI: 0.14–0.18); $P = 0.03$; second order radial arteries: control 0.12 mm (CI: 0.11–0.13) *vs.* chronic hypoxia 0.15 mm (CI: 0.14–0.16); $P = 0.001$) (Fig. 5*C*). The physiological effect of this increase in radial artery diameter is a predicted 2.8-fold decrease in the radial artery resistance (control 5.9 mmHg s $\mu$L$^{-1}$ (CI: 5.1–6.7) *vs.* chronic hypoxia 2.1 mmHg s $\mu$L$^{-1}$ (CI: 1.5–2.7);

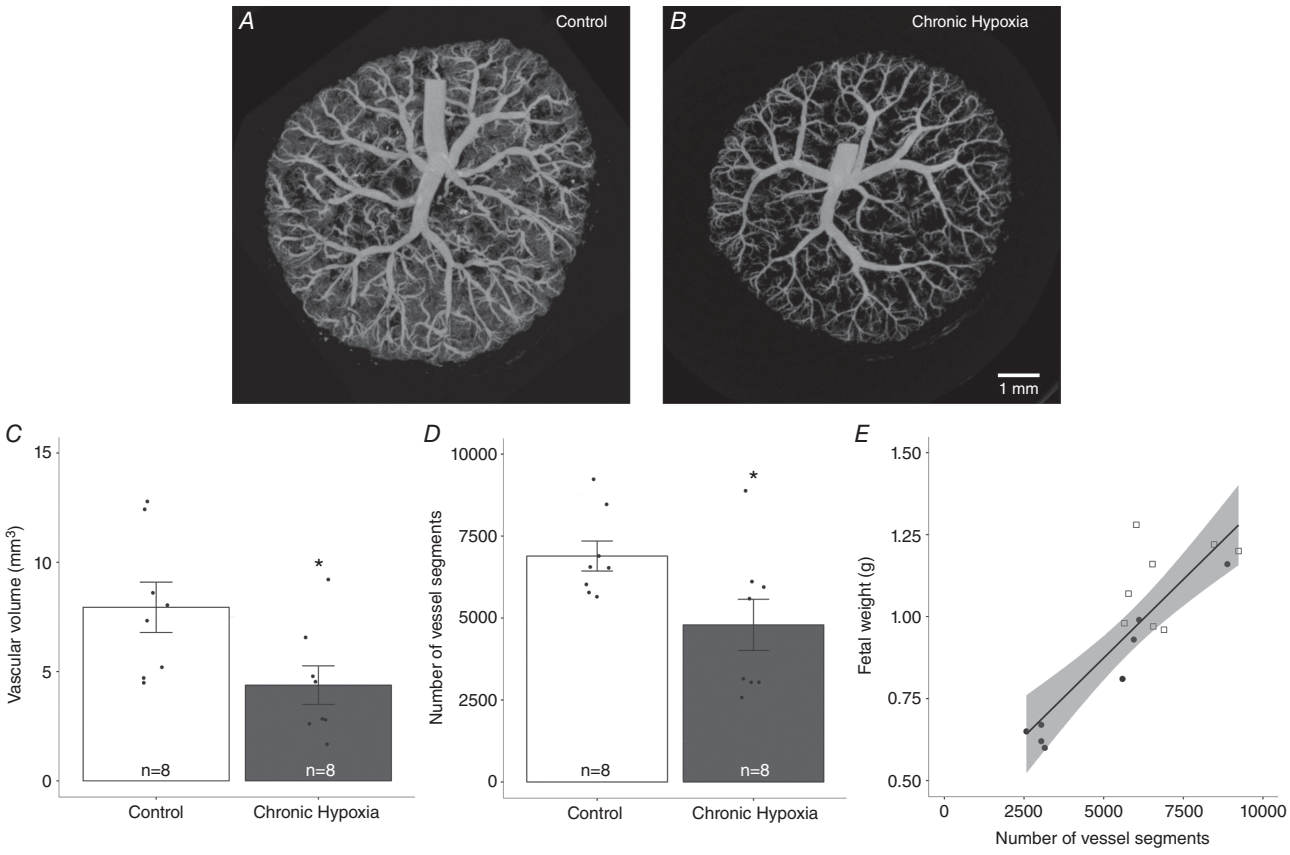


**Figure 3. The effects of chronic maternal hypoxia on the feto-placental arterial vascular tree**
Maximum intensity projection images of example control (*A*) and chronic hypoxia (*B*) feto-placental arterial vascular trees. *C* and *D*, vascular volume (mm$^3$; *C*) and number of vessel segments (*D*) for chronic hypoxia (filled bars) compared to control (open bars) placentas. *E*, fetal weights showed a positive dependence on the total number of vessel segments ($P < 0.0001$, adjusted $R^2 = 0.74$) for the control (open squares) and chronic hypoxia (filled circles) groups. Data shown as means ± 95% confidence intervals. *n* refers to the number of fetuses/placentas. *$P < 0.05$.

$P < 0.0001$). In addition, there was a trend towards a decrease in the resistance of the pre-myometrial radial arteries (control 2.0 mmHg s $\mu L^{-1}$ (CI: 0.7–3.7) *vs.* chronic hypoxia 0.8 mmHg s $\mu L^{-1}$ (CI: 0.3–1.3); $P = 0.06$) and spiral arteries (control 0.6 mmHg s $\mu L^{-1}$ (CI: 0.4–0.8) *vs.* chronic hypoxia 0.4 mmHg s $\mu L^{-1}$ (CI: 0.3–0.5); $P = 0.06$). These changes resulted in a 2.6-fold decrease in total utero-placental vascular resistance in the placentas of mice exposed to chronic maternal hypoxia compared to controls (control 6.5 mmHg s $\mu L^{-1}$ (CI: 5.9–7.1) *vs.* chronic hypoxia 2.6 mmHg s $\mu L^{-1}$ (CI: 2.0–3.2); $P < 0.0001$) (Fig. 5*D*).

## Discussion

Using high-resolution micro-CT and SEM imaging combined with vascular segmentation, we found significant effects of chronic maternal hypoxia on both the feto- and utero-placental circulations. While there was reduced feto-placental arterial expansion in the chronic hypoxia placentas, the capillary network significantly expanded and the interhaemal membrane thinned to increase the surface area and thereby promote enhanced oxygen conductance to the fetus. Similar changes in the fetal capillaries and in the diffusion capacity have been reported with chronic maternal hypoxia in a guinea-pig

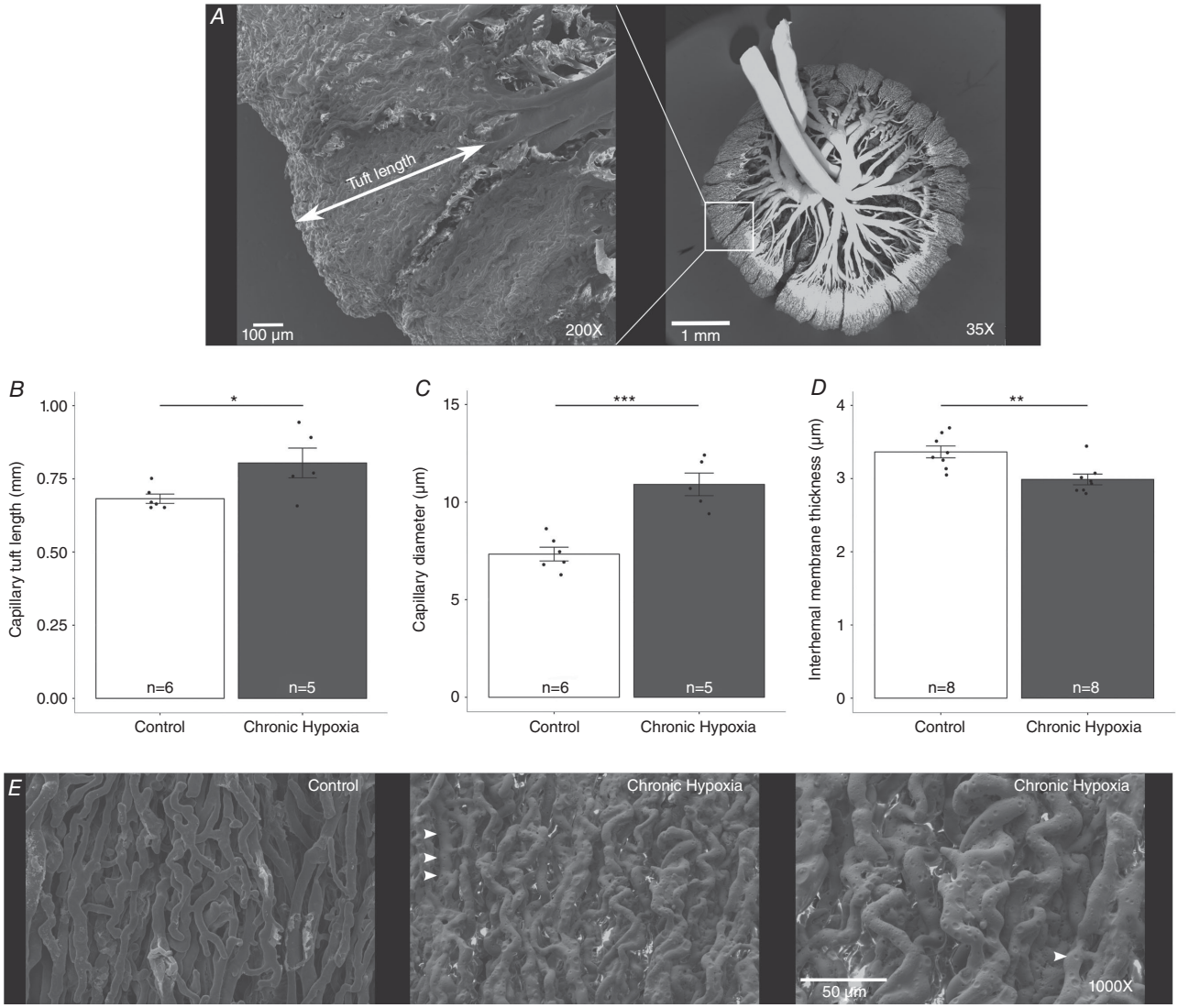


**Figure 4. The effects of chronic maternal hypoxia on the capillary network**
*A*, SEM image of a representative E17.5 control placenta. *B–D*, capillary tuft length (mm; *B*), capillary diameter ($\mu$m; *C*) and interhaemal membrane thickness ($\mu$m; *D*) for chronic hypoxia (filled bars) compared to control (open bars) placentas. *E*, SEM images showing evidence of intussusceptive angiogenesis. Arrowheads in *E* indicate intussusceptive pillars. Data shown as means ± 95% confidence intervals. *n* refers to the number of placentas. $^*P < 0.05$, $^{**}P < 0.005$, $^{***}P < 0.0005$.

model (Bacon *et al.* 1984). In pregnant sheep raised at high altitude, the placenta has also been shown to adapt by increasing the surface area for exchange and increasing the surface occupied by the vasculature (Parraguez *et al.* 2006). Our observations are also consistent with human studies that have reported increased capillarization of the terminal villi and decreased diffusion distance with chronic hypoxia (Alia *et al.* 1996; Mayhew, 1998; Tissot van Patot *et al.* 2003) and with smoking (Pfarrer *et al.* 1999) or anaemia during pregnancy (Kadyrov *et al.* 1998). One of the mechanisms used to achieve the increase in capillaries was intussusceptive angiogenesis. Intussusception has been shown to play an important role in microvascular adaptation in many clinical pathophysiological conditions (Styp-Rekowska *et al.* 2011) and is responsible for the formation of terminal villi in the third trimester of normal human pregnancy. This phenomenon is considered to be energetically and metabolically more effective than sprouting angiogenesis because it does not require an increase in endothelial cells (Djonov *et al.* 2003; Mentzer & Konerding, 2014). Here, evidence for intussusception is consistent with the rapid expansion of the capillary bed required to compensate for the chronic hypoxic environment. Furthermore, vascular endothelial growth factor (VEGF), an important regulator of placental vascular growth, is known to be increased under hypoxia conditions (Forsythe *et al.* 1996) and up-regulation of VEGF is known to promote intussusceptive angiogenesis (Gianni-Barrera *et al.* 2013). It has been shown that intussusceptive angiogenesis is one of the mechanisms that support the rapid growth of the mouse uterus during the post-implantation period, before placental development (Kim *et al.* 2013). To our knowledge, this is the first report of intussusception in the mouse placenta.

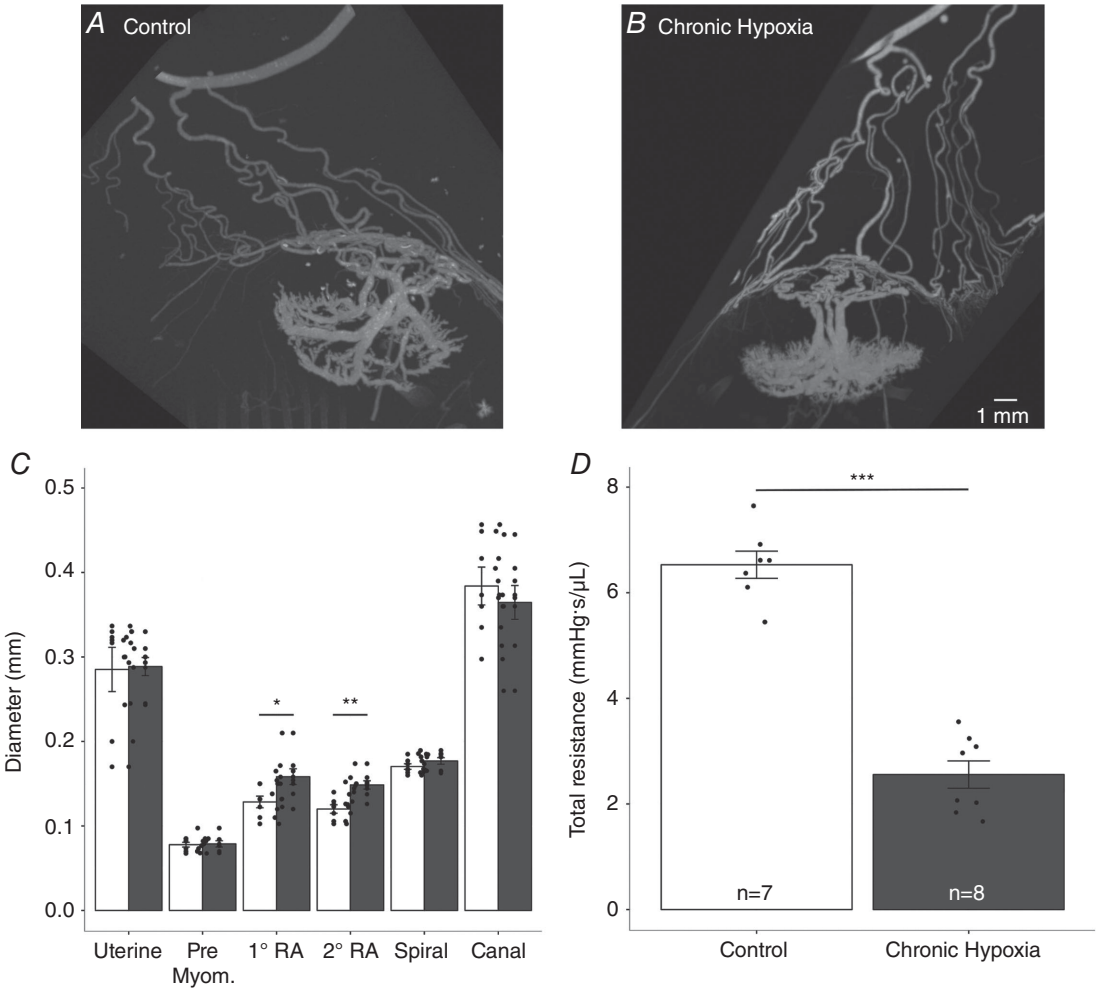


**Figure 5. The effects of chronic maternal hypoxia on the utero-placental arterial vascular tree**
Maximum intensity projection images of example control (*A*) and chronic hypoxia (*B*) utero-placental arterial vascular trees. *C* and *D*, diameter (mm; *C*) and total resistance (mmHg s $\mu L^{-1}$; *D*) for chronic hypoxia (filled bars) compared to control (open bars) placentas. Data shown as means ± 95% confidence intervals. *n* refers to the number of placentas. $^{*}P < 0.05$, $^{**}P < 0.001$, $^{***}P < 0.0001$. Pre Myom., pre-myometrial radial arteries; RA, radial arteries.

The observation that fetal weight increased with the total number of feto-placental vessel segments is consistent with the latter providing a surrogate measure of placental function. Allometric scaling laws for fetal weight have been investigated previously to explain fetal weight differences associated with healthy and pathological placental morphology (Salafia & Yampolsky, 2009). In the present study, with a comparatively small sample size, no difference was observed in this relationship for chronic hypoxia and control placentas.

Observed changes in vascular geometry downstream of the uterine artery, specifically increases in the diameter of the first and second order radial arteries, were estimated to decrease total utero-placental resistance by 2.6-fold in the mice exposed to chronic maternal hypoxia. The large effect of the radial artery adaptation on resistance is consistent with our previous work in normal mouse pregnancies where we showed that the radial arteries have the largest contribution (90% at E17.5) to total utero-placental resistance and total utero-placental pressure drop (Rennie *et al.* 2016), which also appears to be the case in the human utero-placental vasculature network (Burton *et al.* 2009). The current work highlights the important role of the radial arteries in vascular remodelling resulting from late gestation maternal hypoxia. Such changes will deliver greater amounts of oxygen to the labyrinth, where greater fractional oxygen extraction is predicted to occur in the face of the observed adaptive angiogenesis.

The large decrease in utero-placental resistance in the mice exposed to chronic maternal hypoxia would result in a significant increase in blood flow to the exchange region, presumably to compensate for the decreased oxygen content of the maternal blood. It should be noted that the large increase in blood flow through this vascular bed could have potentially deleterious effects on the feto-placental vasculature via mechanical compression. In normal pregnancy, blood pressure at the exchange surface is low (only a few mmHg) and the pressure difference between the maternal and fetal blood is low enough to avoid compression of the feto-placental capillaries (Karimu & Burton, 1994). The pressure drop, while maintaining blood flow, is achieved in human pregnancy by the funnel-shaped spiral arteries (Burton *et al.* 2009). If the pressure drop across the utero-placental arteries is inadequate, the placenta villi may be damaged, as is observed in human pathological pregnancies where arcuate arteries directly enter the placenta, evidenced by the dark intra-placental bands observed in placenta percreta (Balcacer *et al.* 2016). In the present study, despite the large decrease in utero-placental resistance, the SEM images of the capillaries for the chronic hypoxia group did not show evidence of collapse.

In high altitude human pregnancies, there is an increase in the number of spiral arteries (Tissot van Patot *et al.* 2003), but they are less remodelled (Tissot van Patot *et al.* 2003; Zamudio, 2003) and thus overall have an associated lower uterine blood flow (Zamudio *et al.* 1995) compared to normal pregnancies. However, this effect is modulated in multigenerational high altitude residents (Wilson *et al.* 2007). Compared to the present study where we observed the same number of spiral arteries and increased uterine blood flow, the difference may be explained by the fact that the mice are only exposed to hypoxia during late gestation or may reflect interspecies variability in vascular adaptations to chronic hypoxia. In sheep studies exposed to high altitude during late gestation, there was also a rise in utero-placental blood flow (Kitanaka *et al.* 1989; White & Zhang, 2003).

Despite the significant changes in placental vascular morphology, there was no effect of chronic hypoxia on overall placental weight. This is consistent with previous findings in rodents exposed to hypoxia during late gestation (Lueder *et al.* 1995; Saker *et al.* 1999; Cuffe *et al.* 2014). The decrease in placental efficiency observed here is consistent with human fetuses exposed to hypoxia (Macdonald *et al.* 2014) and with a study of rats subjected to hypoxia for most of gestation (Richter *et al.* 2012). While the study by Richter *et al.* reported an increase in placental weights, stereological analysis found no difference in placental volume or compartmental volumes (decidua basalis, junctional zone or labyrinth zone) between chronic hypoxia and control groups. Cuffe *et al.* (2014) reported evidence of placental hypoxia, particularly in the junctional zone. However, using Hypoxyprobe staining, we did not see any significant difference in immunoreactivity between the chronic hypoxia and control groups. The difference may be explained by the longer duration of the chronic hypoxia protocol used by Cuffe *et al.* (4 *vs.* 3 days) or by methodological differences in hypoxia detection; they used Western blot analysis to look at the pimonidazole adducts in the placental tissue as well as HIF1A immunolabelling to look for evidence of increased placental hypoxia relative to controls. An alternate explanation is that increases in feto-placental capillary volumes are offset by changes more proximal in the placental vascular tree. Interestingly, the umbilical cord was significantly shorter in the chronic hypoxia group in the present study. In humans, short umbilical cords are loosely correlated with decreased fetal growth, amniotic fluid volume and fetal movement (Miller *et al.* 1981) and have been associated with fetal compromise (Krakowiak *et al.* 2004).

The present study has several limitations. One is that the sex of the fetus was not determined. Recent evidence suggests that placental adaptations to chronic maternal hypoxia are sex dependent (Cuffe *et al.* 2014) and it is possible that some of the variability in our measurements could have been the result of sex differences. The food intake of the dams exposed to chronic hypoxia was not recorded. This may partially explain the lack of

maternal weight gain; however, a recent study found no change in maternal food intake in response to chronic hypoxia (Cuffe *et al.* 2014). Another limitation is that each of the experimental assays (feto-placental perfusion, utero-placental perfusion, methyl methacrylate perfusion) required a separate cohort, preventing us from examining correlations within specimens. Finally, all measurements were obtained from *ex vivo* imaging of perfused specimens. While previous work in our group has shown close agreement between these measurements and those obtained *in vivo* by ultrasound (Rennie *et al.* 2007), this approach does not reproduce the pressure gradient in the vessels that would be present with flowing blood.

In summary, the use of experimental mice allowed us to investigate the changes in the microcirculation of the placenta with chronic maternal hypoxia. In response to a chronic hypoxic environment, there were several adaptations in the placenta that were beneficial to fetal growth including capillary expansion, thinning of the interhaemal membrane and expansion of the diameter of the radial arteries to increase utero-placental blood flow. These results provide a baseline for adaptive physiological responses to chronic hypoxia and can be used to identify when compensatory mechanisms fail due to pathological conditions.

## References


Alia KZM, Burton GJ, Morad N & Ali ME (1996). Does hypercapillarization influence the branching pattern of terminal villi in the human placenta at high altitude. *Placenta* **17**, 677–682.

Bacon BJ, Gilbert RD, Kaufmann P, Smith AD, Trevino FT & Longo LD (1984). Placental anatomy and diffusing capacity in guinea pigs following long-term maternal hypoxia. *Placenta* **5**, 475–488.

Bainbridge SA, Minhas A, Whiteley KJ, Qu D, Sled JG, Kingdom JC & Adamson SL (2012). Effects of reduced Gcm1 expression on trophoblast morphology, fetoplacental vascularity, and pregnancy outcomes in mice. *Hypertension* **59**, 732–739.

Balcacer P, Pahade J, Spektor M, Staib L, Copel JA & McCarthy S (2016). Magnetic resonance imaging and sonography in the diagnosis of placental invasion. *J Ultrasound Med* **35**, 1445–1456.

Boddy K, Dawes GS, Fisher R, Pinter S & Robinson JS (1974). Foetal respiratory movements, electrocortical and cardiovascular responses to hypoxaemia and hypercapnia in sheep. *J Physiol* **243**, 599–618.

Bohlen HG & Gore RW (1977). Comparison of microvascular pressures and diameters in the innervated and denervated rat intestine. *Microvasc Res* **14**, 251–264.

Burton GJ, Woods AW, Jauniaux E & Kingdom JCP (2009). Rheological and physiological consequences of conversion of the maternal spiral arteries for uteroplacental blood flow during human pregnancy. *Placenta* **30**, 473–482.

Coan PM, Angiolini E, Sandovici I, Burton GJ, Constancia M & Fowden AL (2008). Adaptations in placental nutrient transfer capacity to meet fetal growth demands depend on placental size in mice. *J Physiol* **586**, 4567–4576.

Coan PM, Ferguson-Smith AC & Burton GJ (2004). Developmental dynamics of the definitive mouse placenta assessed by stereology. *Biol Reprod* **70**, 1806–1813.

Cohn HE, Sacks EJ, Heymann MA & Rudolph AM (1974). Cardiovascular responses to hypoxemia and acidemia in fetal lambs. *Am J Obstet Gynecol* **120**, 817–824.

Cox B, Kotlyar M, Evangelou AI, Ignatchenko V, Ignatchenko A, Whiteley K, Jurisica I, Adamson SL, Rossant J & Kislinger T (2009). Comparative systems biology of human and mouse as a tool to guide the modeling of human placental pathology. *Mol Syst Biol* **5**, 279.

Cuffe JSM, Walton SL, Singh RR, Spiers JG, Bielefeldt-Ohmann H, Wilkinson L, Little MH & Moritz KM (2014). Mid- to late term hypoxia in the mouse alters placental morphology, glucocorticoid regulatory pathways and nutrient transporters in a sex-specific manner. *J Physiol* **14**, 3127–3141.

Djonov V, Baum O & Burri PH (2003). Vascular remodeling by intussusceptive angiogenesis. *Cell Tissue Res* **314**, 107–117.

Forsythe JA, Jiang BH, Iyer NV, Agani F, Leung SW, Koos RD & Semenza GL (1996). Activation of vascular endothelial growth factor gene transcription by hypoxia-inducible factor 1. *Mol Cell Biol* **16**, 4604–4613.

Georgiades P, Ferguson-Smith AC & Burton GJ (2002). Comparative developmental anatomy of the murine and human definitive placentae. *Placenta* **23**, 3–19.

Gianni-Barrera R, Trani M, Fontanellaz C, Heberer M, Djonov V, Hlushchuk R & Banfi A (2013). VEGF over-expression in skeletal muscle induces angiogenesis by intussusception rather than sprouting. *Angiogenesis* **16**, 123–126.

Giussani DA (2016). The fetal brain sparing response to hypoxia: physiological mechanisms. *J Physiol* **594**, 1215–1230.

Gleason CA, Hamm C & Jones MD (1990). Effect of acute hypoxemia on brain blood flow and oxygen metabolism in immature fetal sheep. *Am J Physiol Heart Circ Physiol* **258**, H1064–H1069.

Gortner L, Hilgendorff A, Bähner T, Ebsen M, Reiss I & Rudloff S (2005). Hypoxia-induced intrauterine growth retardation: effects on pulmonary development and surfactant protein transcription. *Biol Neonate* **88**, 129–135.

Hayward CE, Lean S, Sibley CP, Jones RL, Wareing M, Greenwood SL & Dilworth MR (2016). Placental adaptation: what can we learn from birthweight: placental weight ratio? *Front Physiol* **7**, 28.

Higgins JS, Vaughan OR, Liger E, Fowden AL & Sferruzzi-Perri AN (2016). Placental phenotype and resource allocation to fetal growth are modified by the timing and degree of hypoxia during mouse pregnancy. *J Physiol* **594**, 1341–1356.

Jang EA, Longo LD & Goyal R (2015). Antenatal maternal hypoxia: criterion for fetal growth restriction in rodents. *Front Physiol* **6**, 176.

Kadyrov N, Kosanke G, Kingdom J & Kaufmann P (1998). Increased fetoplacental angiogenesis during first trimester in anaemic women. *The Lancet* **352**, 1747–1749.

Karimu AL & Burton GJ (1994). The effects of maternal vascular pressure on the dimensions of the placental capillaries. *Br J Obstet Gynaecol* **101**, 57–63.

Kim M, Park HJ, Seol JW, Jang JY, Cho YS, Kim KR, Choi Y, Lydon JP, Demayo FJ, Shibuya M, Ferrara N, Sung HK, Nagy A, Alitalo K & Koh GU (2013). VEGF-A regulated by progesterone governs uterine angiogenesis and vascular remodelling during pregnancy. *EMBO Mol Med* **5**, 1415–1430.

Kingdom JCP & Kaufmann P (1997). Oxygen and placental villous development: origins of fetal hypoxia. *Placenta* **18**, 613–621.

Kitanaka T, Gilbert RD & Longo LD (1989). Maternal responses to long-term hypoxemia in sheep. *Am J Physiol Regul Integr Comp Physiol* **256**, R1340–R1347.

Krakowiak P, Smith EN, de Bruyn G & Lydon-Rochelle MT (2004). Risk factors and outcomes associated with a short umbilical cord. *Obstet Gynecol* **103**, 119–127.

Kulandavelu S, Whiteley KJ, Bainbridge SA, Qu D & Adamson SL (2013). Endothelial NO synthase augments fetoplacental blood flow, placental vascularization, and fetal growth in mice. *Hypertension* **61**, 259–266.

Lueder FL, Kim SB, Buroker CA, Bangalore SA & Ogata ES (1995). Chronic maternal hypoxia retards fetal growth and increases glucose utilization of select fetal tissues in the rat. *Metabolism* **44**, 532–537.

Lyall F (2005). Priming and remodelling of human placental bed spiral arteries during pregnancy – a review. *Placenta* **26**, S31–S36.

Macdonald EM, Natale R, Regnault TRH, Koval JJ & Campbell MK (2014). Obstetric conditions and the placental weight ratio. *Placenta* **35**, 582–586.

Martin CB (2008). Normal fetal physiology and behavior, and adaptive responses with hypoxemia. *Semin Perinatol* **32**, 239–242.

Mayhew TM (1998). Thinning of the intervascular tissue layers of the human placenta is an adaptive response to passive diffusion in vivo and may help to predict the origins of fetal hypoxia. *Eur J Obstet Gynecol Reprod Biol* **81**, 101–109.

Mentzer SJ & Konerding MA (2014). Intussusceptive angiogenesis: expansion and remodeling of microvascular networks. *Angiogenesis* **17**, 499–509.

Miller ME, Higginbottom M & Smith DW (1981). Short umbilical cord: its origin and relevance. *Pediatrics* **67**, 618–621.

Moore LG, Shriver M, Bemis L, Hickler B, Wilson M, Brutsaert T, Parra E & Vargas E (2004). Maternal adaptation to high-altitude pregnancy: an experiment of nature – a review. *Placenta* **25**, S60–S71.

Mu J & Adamson SL (2006). Developmental changes in hemodynamics of uterine artery, utero-and umbilicoplacental, and vitelline circulations in mouse throughout gestation. *Am J Physiol Heart Circ Physiol* **291**, H1421–H1428.

Parraguez VH, Atlagich M, Díaz R, Cepeda R, Gonzalez C, De los Reyes M, Bruzzone ME, Behn C & Raggi LA (2006). Ovine placenta at high altitudes: Comparison of animals with different times of adaptation to hypoxic environment. *Anim Reprod Sci* **95**, 151–157.

Pearce W (2006). Hypoxic regulation of the fetal cerebral circulation. *J Appl Physiol* **100**, 731–738.

Perry IJ, Beevers DG, Whincup PH & Bareford D (1995). Predictors of ratio of placental weight to fetal weight in multiethnic community. *BMJ* **310**, 436–439.

Pfarrer C, Macara L, Leiser R & Kingdom J (1999). Adaptive angiogenesis in placentas of heavy smokers. *Lancet* **24**, 303.

Ream M, Ray AM, Chandra R & Chikaraishi DM (2008). Early fetal hypoxia leads to growth restriction and myocardial thinning. *Am J Physiol Regul Integr Comp Physiol* **295**, R583–R595.

Rennie MY, Detmar J, Whiteley KJ, Jurisicova A, Adamson SL & Sled JG (2012). Expansion of the fetoplacental vasculature in late gestation is strain dependent in mice. *Am J Physiol Heart Circ Physiol* **302**, H1261–H1273.

Rennie MY, Detmar J, Whiteley KJ, Yang J, Jurisicova A, Adamson SL & Sled JG (2011). Vessel tortuousity and reduced vascularization in the fetoplacental arterial tree after maternal exposure to polycyclic aromatic hydrocarbons. *Am J Physiol Heart Circ Physiol* **300**, H675–H684.

Rennie MY, Rahman A, Whiteley KJ, Sled JG & Adamson SL (2015). Site-specific increases in utero-and fetoplacental arterial vascular resistance in eNOS-deficient mice due to impaired arterial enlargement. *Biol Reprod* **92**, 1–11.

Rennie MY, Sled JG & Adamson SL (2014*a*). Effects of genes and environment on the fetoplacental arterial microcirculation in mice revealed by micro-computed tomography imaging. *Microcirculation* **21**, 48–57.

Rennie MY, Whiteley KJ, Adamson SL & Sled JG (2016). Quantification of gestational changes in the uteroplacental vascular tree reveals vessel specific hemodynamic roles during pregnancy in mice. *Biol Reprod* **95**, 1–9.

Rennie MY, Whiteley KJ, Kulandavelu S, Adamson SL & Sled JG (2007). 3D visualisation and quantification by microcomputed tomography of late gestational changes in the arterial and venous feto-placental vasculature of the mouse. *Placenta* **28**, 833–840.

Rennie MY, Whiteley KJ, Sled JG & Adamson SL (2014*b*). Scanning electron microscopy and micro-computed tomography imaging of the utero- and fetoplacental circulations. In *The Guide to Investigation of Mouse Pregnancy*, eds Croy BA, Yamada AT, DeMayo FJ & Adamson SL, pp. 637–648. Elsevier.

Richter HG, Camm EJ, Modi BN, Naeem F, Cross CM, Cindrova-Davies T, Spasic-Boskovic O, Dunster C, Mudway IS, Kelly FJ, Burton GJ & Poston L (2012). Ascorbate prevents placental oxidative stress and enhances birth weight in hypoxic pregnancy in rats. *J Physiol* **590**, 1377–1387.

Rueda-Clausen CF, Stanley JL, Thambiraj DF, Poudel R, Davidge ST & Baker PN (2014). Effect of prenatal hypoxia in transgenic mouse models of preeclampsia and fetal growth restriction. *Reprod Sci* **21**, 492–502.

Saker F, Voora DM, Mahajan SD, Kiliç Í, Ismail-Beigi F & Kalhan SC (1999). Effect of reduced inspired oxygen on fetal growth and maternal glucose metabolism in rat pregnancy. *Metabolism* **48**, 738–744.

Salafia CM & Yampolsky M (2009). Metabolic scaling law for fetus and placenta. *Placenta* **30**, 468–471.

Styp-Rekowska B, Hlushchuk R, Pries AR & Djonov V (2011). Intussusceptive angiogenesis: pillars against the blood flow. *Acta Physiol (Oxf)* **202**, 213–223.

Tissot van Patot M, Grilli A, Chapman P, Broad E, Tyson W, Heller DS & Zwerdlinger L (2003). Remodelling of uteroplacental arteries is decreased in high altitude placentae. *Placenta* **24**, 326–335.

Tomlinson TM, Garbow JR, Anderson JR, Engelbach JA, Nelson DM & Sadovsky Y (2010). Magnetic resonance imaging of hypoxic injury to the murine placenta. *Am J Physiol Regul Integr Comp Physiol* **298**, R312–R319.

White MM & Zhang L (2003). Effects of chronic hypoxia on maternal vasodilation and vascular reactivity in guinea pig and ovine pregnancy. *High Alt Med Biol* **4**, 157–169.

Whiteley KJ, Pfarrer CD & Adamson SL (2006). Vascular corrosion casting of the uteroplacental and fetoplacental vasculature in mice. *Methods Mol Med* **121**, 371–392.

Wilson MJ, Lopez M, Vargas M, Julian C, Tellez W, Rodriguez A, Bigham A, Armaza JF, Niermeyer S, Shriver M, Vargas E & Moore LG (2007). Greater uterine artery blood flow during pregnancy in multigenerational (Andean) than shorter-term (European) high-altitude residents. *Am J Physiol Regul Integr Comp Physio* **293**, R1313–R1324.

Zamudio S (2003). The placenta at high altitude. *High Alt Med Biol* **4**, 171–191.

Zamudio S, Palmer SK, Droma T, Stamm E, Coffin C & Moore LG (1995). Effect of altitude on uterine artery blood flow during normal pregnancy. *J Appl Physiol* **79**, 7–14.

## Additional information

### Competing interests

The authors declare that they have no competing interests.

### Author contributions

L.S.C. wrote the manuscript. L.S.C., M.Y.R., L.X.Y. and A.R. acquired the experimental data. L.S.C., M.Y.R. and J.H. performed the analysis and interpretation of the data. L.S.C., M.Y.R., J.K., M.S., C.K.M. and J.G.S. conceived of the study and are responsible for the overall design of the research. All of the authors approved of the final version of the manuscript and agree to be accountable for all aspects of the work. All persons designated as authors qualify for authorship, and all those who qualify for authorship are listed.

### Funding

This work was supported by the Eunice Kennedy Shriver National Institute of Child Health & Human Development (NICHD) Office of The Director, National Institutes of Health (OD) (1U01HD087177) and the Canadian Institutes of Health Research (MOP 130403).